Composition and Sequence Specific Resonance Assignments of the Heterogeneous *N*-Linked Glycan in the 13.6 kDa Adhesion Domain of Human CD2 as Determined by NMR on the Intact Glycoprotein†

Daniel F. Wyss,‡,§ Johnathan S. Choi,‡ and Gerhard Wagner*,‡

Department of Biological Chemistry and Molecular Pharmacology, Harvard Medical School, Boston, Massachusetts 02115

Received October 18, 1994; Revised Manuscript Received December 1, 1994⊗

ABSTRACT: CD2, a T cell specific surface adhesion receptor, is critically important for T lymphocytes to mediate their regulatory and effector functions. The amino terminal domain of human CD2 is responsible for cell adhesion, binding to CD58 on antigen-presenting cells or target cells. This adhesion domain in human CD2 contains a single high-mannose *N*-glycan. This carbohydrate or part of it appears to be required to maintain the native conformation of the polypeptide and its ability to bind CD58. To better understand the structural aspects that regulate human CD2 adhesion functions, we had previously determined the solution structure of the protein part of the *N*-glycosylated adhesion domain of human CD2 (hu-$sCD2_{105}$; MW ~ 13.6 kDa) by NMR spectroscopy. Here, we have identified protein−carbohydrate and carbohydrate−carbohydrate interactions and, in combination with previous knowledge from electrospray ionization mass spectrometry, have determined the composition of the heterogeneous high-mannose glycan in hu-$sCD2_{105}$. These contacts clearly define the carbohydrate's orientation with respect to the protein. The NMR data further suggest that one arm of the glycan is folded toward the trisaccharide core consisting of GlcNAc1-GlcNAc2-Man3. A detailed comparison between chemical shift data of free model oligosaccharides with those of the glycomers present in our hu-$sCD2_{105}$ sample reveals that only the resonances of the two GlcNAc residues are significantly different from those of free high-mannose glycans. This work was based on a new strategy to achieve sequential assignments of the ^1H and ^{13}C resonances of the heterogeneous high-mannose carbohydrate [$(Man)_nGlcNAc_2$, $n = 5-8$] in hu-$sCD2_{105}$ on the intact glycoprotein using a combination of homonuclear $^1H-^1H$ and heteronuclear $^1H-^{13}C$ NMR experiments at natural abundance.

T cells express a distinct array of cell surface receptors which are responsible for the highly specific recognition of and response to foreign antigens. Adhesion is mediated by specific interactions of cell surface adhesion receptors with counter receptors, carbohydrates or proteins from the extracellular matrix (Pigott & Power, 1993; Wagner & Wyss, 1994). In recent years large numbers of cell adhesion molecules (CAMs) have been identified on leukocytes (Barclay et al., 1993). CD2,[1] an invariant 50−55 kDa surface glycoprotein which is found on virtually all T lymphocytes as well as on natural killer cells, initiates the adhesion of T lymphocytes to infected target cells and antigen-presenting cells (APCs) (Bierer et al., 1988; Moingeon et al., 1989a; Koyasu et al., 1990) prior to up-regulation of other receptor-mediated adhesion pathways (Dustin & Springer, 1991; Moingeon et al., 1991), thereby promoting maximally effective interactions between these cells [reviewed in Moingeon et al. (1989b), Bierer et al. (1989), Bromberg (1993), Hahn et al. (1993)].

In humans, CD2 binds specifically to CD58 (LFA-3) expressed on the surface of APCs and epithelial, endothelial, and target cells of various types (Shaw et al., 1986; Selvaraj et al., 1987). The membrane distal amino terminal domains of human CD2 and human CD58 bind to one another with a micromolar affinity (Sayre et al., 1989; Recny et al., 1990; Miller et al., 1993). This modest, monomeric binding activity is amplified by multimeric interaction at the cell−cell interface resulting from rapid redistribution of CD2 to the intercellular junction (Koyasu et al., 1990; Moingeon et al., 1991). Anti-CD2 monoclonal antibodies which inhibit CD58 binding can block conjugate formation between T cells and other CD58-expressing cells, leading to suppression of cellular-mediated immune responses (Meuer et al., 1984; Bierer et al., 1988). Furthermore, blocking CD2−CD58 interactions between T cells and APCs with a soluble version of the human CD2 extracellular domain can also effectively suppress both memory T cell responses to recall antigens and alloreactive responses (Rabin et al., 1993). In contrast, in rodents the only known ligand for CD2 is CD48 (van der

† This work was supported by NIH (Grants GM38608 and GM47467), the Keck Foundation, and grants from Procept, Inc. and Sandoz Pharma Ltd. to D.F.W.

‡ Harvard Medical School.

§ Procept, Inc., 840 Memorial Dr., Cambridge, MA 02139.

⊗ Abstract published in *Advance ACS Abstracts,* January 15, 1995.

[1] Abbreviations: APC, antigen-presenting cell; CD2, cluster of differentiation 2; CHO cells, Chinese hamster ovary cells; DEPT, distortionless enhancement by polarization transfer; DIPSI, decoupling in the presence of scalar interactions; EASY, *E*TH *a*utomated *sy*stroscopy; ESI-MS, electrospray ionization mass spectrometry; GlcNAc, *N*-acetylglucosamine; HMBC, heteronuclear multiple-bond correlation; HMQC, heteronuclear multiple quantum correlation; IgSF, immunoglobulin superfamily; LFA-3, lymphocyte function-associated antigen-3; mAbs, monoclonal antibodies; Man, mannose; NMR, nuclear magnetic resonance; NOESY, nuclear Overhauser enhancement spectroscopy; ppm, parts per million; SCUBA, stimulated cross-peaks under bleached alphas; TOCSY, total correlation spectroscopy; TPPI, time-proportional phase incrementation; TQF-COSY, triple-quantum-filtered correlated spectroscopy; TSP, sodium 3-(trimethylsilyl)propionate; V-set IgSF domain, immunoglobulin variable domain; hu-$sCD2_{182}$, two-domain 182-amino acid glycosylated extracellular segment of human CD2; hu-$sCD2_{105}$, amino terminal 105-amino acid *N*-glycosylated adhesion domain of human CD2; 2D, two dimensional; 3D, three dimensional.

0006-2960/95/0434-1622$09.00/0

Merwe et al., 1993a; Kato et al., 1992), and no gene for CD58 has been identified in these species. Human CD2 also binds the structurally homologous CD48, but the affinity is 2 orders of magnitude weaker ($K_d = 10^{-4}$ M) than that of the CD2−CD58 interaction and, hence, is unable to support cell adhesion in an *in vitro* assay (Arulanandam et al., 1993a). Although there have been reports suggesting that CD59 is an alternative ligand for human CD2 whose binding site overlaps with CD58 (Hahn et al., 1992; Deckert et al., 1992), other evidence directly contradicts these findings (Arulanandam et al., 1993a). Using surface plasmon resonance technology, binding affinities and dissociation rate constants were recently obtained on the interactions of rat CD2 with rat CD48 (van der Merwe et al., 1993b), as well as of human CD2 with human CD58, human CD48, and human CD59 (van der Merwe et al., 1994). For the CD2−CD58 and CD2−CD48 interactions in humans and rat, respectively, very low affinities [$K_d = 9-22$ μM (hCD2−hCD58); $K_d = 60-90$ μM (rCD2−rCD48)] and extremely fast dissociation rates [$k_{off} \geq 4$ s^{-1} (hCD2−hCD58); $k_{off} \geq 6$ s^{-1} (rCD2−rCD48)] were observed, and no direct interaction between CD2 and either CD48 or CD59 was detected in humans (van der Merwe et al., 1994).

In addition to its adhesive function, CD2 has been shown capable of transducing activation signals, whereby ligation of the CD2 extracellular domains by CD58 or a combination of monoclonal antibodies which bind specific epitopes in both domains 1 and 2 can lead to activation of T cells independent of antigen recognition by the T cell receptor (TCR) (Meuer et al., 1984; Siliciano et al., 1985; Yang et al., 1986; Hünig et al., 1987). Furthermore, *in vivo* studies have shown that a combination of either anti-CD2 receptor and anti-CD2 ligand or anti-CD2 and anti-CD3 receptor monoclonal antibodies (mAbs) produce indefinite graft survival in cardiac allograft models (Chavin et al., 1993; Qin et al., 1994).

Human CD2 is a member of the immunoglobulin superfamily (IgSF) (Williams & Barclay, 1988; Williams et al., 1989) and consists of a two-domain 185-amino acid residue extracellular segment, a 25-residue hydrophobic transmembrane-spanning region, and a 117-residue cytoplasmic tail (Sewell et al., 1986; Sayre et al., 1987; Clayton et al., 1987) which is required for CD2-mediated signal transduction (He et al., 1988; Chang et al., 1989). All adhesion functions have been mapped to the extracellular amino terminal 105-residue domain of human CD2 (Recny et al., 1990) which contains a single consensus *N*-glycosylation site at Asn65 that is occupied with high-mannose oligosaccharides [$(Man)_n$-$GlcNAc_2$, $n = 5-8$] when a soluble version of the CD2 extracellular segment is expressed in Chinese hamster ovary (CHO) cells (Recny et al., 1992). This adhesion domain of human CD2 requires a single *N*-linked carbohydrate to maintain its native conformation and ability to bind CD58 (Recny et al., 1992).

We recently initiated the investigation of the solution structure of the glycosylated adhesion domain of human CD2 (hu-$sCD2_{105}$, MW ~ 13.6 kDa) by nuclear magnetic resonance (NMR) spectroscopy (Wyss et al., 1993) to better understand the structural aspects that regulate human CD2 adhesion functions. It consists of a nine-stranded V-set IgSF domain lacking the first half of strand A (Withka et al., 1993). However, the polypeptide structure of the glycosylated adhesion domain of human CD2 is very similar to that of nonglycosylated rat CD2 domain 1 expressed in *Escherichia coli* (Driscoll et al., 1991) or to those of domain 1 of the two-domain crystal structures of human (Bodian et al., 1994) and rat CD2 (Jones et al., 1992). In the latter two cases the proteins were expressed in CHO cells in the presence of a glucosidase I inhibitor and in a CHO cell glycosylation mutant, respectively, which in both cases produced truncated *N*-linked oligosaccharides that were trimmed by endoglycosidase H resulting in proteins with single *N*-acetylglucosamine (GlcNAc) residues at each glycosylation site.

Upon the basis of detailed analysis of the hu-$sCD2_{105}$ structure, we have also made additional alanine substitution mutations in human CD2 to further probe the apparent binding site for CD58 (Arulanandam et al., 1993b). The latter is a flat and highly charged surface area with an excess of positive charges on the solvent-exposed surface of the GFCC′C″ face of the CD2 β-barrel (Arulanandam et al., 1993b; Somoza et al., 1993). In contrast, the single *N*-linked glycosylation site in hu-$sCD2_{105}$ is located at the top of the DE loop in the opposite solvent-exposed face of the β-barrel, and thus, it is unlikely that the carbohydrate directly interacts with CD58 (Wyss et al., 1993; Withka et al., 1993). Important parts of this receptor interface are the FG, CC′, and C′C″ loops as well as the two β-bulges at the beginning of the G and C′ strands. This is reminiscent of the interactions of the heavy and light chains in immunoglobulins where residues located on β-bulges are also important for the intersubunit interaction (Chothia et al., 1985). Interestingly, the same surface area identified as the receptor interface forms a homodimeric contact in the crystal structures of rat (Jones et al., 1992) and human CD2 (Bodian et al., 1994). Thus, this crystal contact may be a valid model for the complex between the receptor and the counter-receptor CD58.

On the basis of the coordinates of a refined NMR structure of hu-$sCD2_{105}$ (D. Wyss, J. Choi, M. Knoppers, M. Recny, and G. Wagner, personal communications) and the homology between human CD58, human CD2, and other cell surface adhesion receptors, we recently built a model for the adhesion domain of human CD58 (Arulanandam et al., 1994). This model was then used to identify the CD2 binding site of human CD58 by mutating charged residues shared among CD2 ligands (human CD58, sheep CD58, and human CD48) that were predicted to be solvent exposed on this model of human CD58. From these studies it was predicted that the CD2 binding site on CD58 also involves the GFCC′C″ surface, and two possible docking orientations for the CD58−CD2 interaction were created (Arulanandam et al., 1994) on the basis of the CD8 $\alpha-\alpha$-homodimer structure (Leahy et al., 1992) and the head-to-head interaction of symmetry-related molecules in the rat CD2 crystals (Jones et al., 1992). The analysis of this complex offers molecular insight into the nature of a receptor−ligand pair involving two IgSF members.

Detailed structural studies of glycoproteins by either NMR spectroscopy or X-ray crystallography are scarce, primarily due to the heterogeneity, flexibility, and diversity of the attached glycans. These features which are often biologically important for the glycoprotein make a structural characterization of the attached oligosaccharides by spectroscopic methods very difficult. A fundamental problem in applying NMR to the analysis of protein-linked carbohydrate conformations is the difficulty in completely assigning each resonance in the proton spectra because of severe overlap

in the bulk region (3.5−4.0 ppm) (Vliegenthart et al., 1983; Homans, 1990) where many H^{α} and H^{β} of the protein also resonate. The chemical shift dispersion of ^{13}C resonances is much more favorable in oligosaccharides, but to take advantage of this fact, the protein-linked glycans should either be isotopically enriched with ^{13}C or, at the least, the glycoprotein should be soluble at higher concentrations to allow more advanced heteronuclear NMR techniques at natural abundance.

Here we report the sequential ^{1}H and ^{13}C NMR assignments of hu-sCD2$_{105}$ obtained primarily by homonuclear 2D NMR experiments in combination with $^{1}H-^{13}C$ HMQC and $^{1}H-^{13}C$ DEPT-HMQC spectra acquired at natural abundance. To our knowledge, this is the first time that ^{1}H and ^{13}C resonance assignments have been obtained to such an extent for both the protein and glycan components of an intact glycoprotein of this size. Previous conformational studies of intact glycoproteins by NMR have concentrated on either the protein spectrum (Veitch et al., 1992; Kieffer et al., 1994) or the carbohydrate component (Brockbank & Vogel, 1990) or have been limited to glycosylated peptides (Wormald et al., 1991). In a recent analysis of the glycoprotein CD59, Fletcher et al. (1994) achieved partial ^{1}H assignments of the complex type *N*-glycan in CD59 and used NOEs between the GlcNAc1 residue and several protein residues to calculate truncated disaccharide−protein and trisaccharide−protein structures. In contrast to CD2, the carbohydrate in all these cases was not found to be important for the function of the glycoprotein and only limited interactions between the protein and the attached glycans were observed. We have used our extensive set of protein and sugar ^{1}H NMR assignments to specifically look for protein−carbohydrate interactions in hu-sCD2$_{105}$. Only the first two GlcNAc residues appear to make NOE contacts to the protein, and together with mannose 3 (Man3) their resonances show clearly broader line widths than resonances of the remainder of the *N*-linked glycan and similar to the polypeptide signals indicating their restricted mobility. In addition, we characterized the different components of the heterogeneous high-mannose glycan present in our sample.

EXPERIMENTAL PROCEDURES

Protein expression, purification, and sample preparation are described in Wyss et al. (1993). All NMR experiments were performed in 95% (v/v) H_2O/D_2O or D_2O on submillimolar hu-sCD2$_{105}$ samples. Acquired 2D $^{1}H-^{1}H$ NMR data included TOCSY (Braunschweiler & Ernst, 1983) and NOESY (Jeener et al., 1979; Anil-Kumar et al., 1980). Experiments were carried out on either Bruker AMX600 or AMX500 spectrometers with ^{1}H resonance frequencies of 600.13 and 500.13 MHz, respectively. Most experiments were performed at 25 and 37 °C to resolve accidental overlaps. All spectra were recorded in a phase-sensitive manner using the time-proportional phase incrementation method for sign discrimination in the F1 dimension (Marion & Wüthrich, 1983). Spectral widths in the ^{1}H dimension(s) were 8772 and 7246 Hz for the AMX600 and AMX500 spectrometers, respectively. Typically, the spectra were obtained with 512 real points along t_1 (TPPI) and 2048 complex points along t_2. ^{1}H chemical shifts (δ) were referenced relative to internal TSP. The ^{1}H carrier was placed on the H_2O or residual DHO resonance. The water resonance was suppressed by low-power presaturation during the recycle delay (1.0−1.3 s) which in the H_2O samples was followed by the SCUBA sequence using 30 ms delays to recover saturated proton resonances under the water line (Brown et al., 1988). For the NOESY experiments, solvent peak recovery was reduced by inclusion of a 180° composite pulse in the center of the mixing period, and mixing times (τ_m) of 38, 76, 100, and 200 ms were used. A total of 512 t_1 values were collected per mixing time with 256 scans acquired for each t_1 value. All TOCSY spectra were acquired using the DIPSI-2 (Shaka et al., 1988) spin−lock sequence. In the H_2O samples they were recorded with three different mixing times of 32, 55, and 85 ms, which were coadded to a single file, and in the D_2O samples they were acquired with single mixing times of 50, 100, 125, 150, 200, and 250 ms. A total of 512 t_1 values were collected per mixing time with 72 and 16 scans acquired for each t_1 value for the H_2O and D_2O samples, respectively. The 125 ms TOCSY was acquired with 64 scans per t_1 value using the DIPSI-2rc sequence for suppression of cross-relaxation effects (Cavanagh & Rance, 1992).

2D $^{13}C-^{1}H$ HMQC (Mueller, 1979) and 2D $^{13}C-^{1}H$ DEPT-HMQC (Kessler et al., 1989) spectra were recorded at 25 and 37 °C at natural abundance on a 1 mM hu-sCD2$_{105}$ sample in D_2O. The HMQC spectrum was acquired on a AMX600 spectrometer with a ^{13}C frequency of 150.9 MHz, and to increase the sensitivity the ^{13}C spectral width was set to 10 000 Hz around the carrier position at 73 ppm relative to internal TSP which resulted in folding of the aromatic and most side chain carbon resonances of the protein. Defocusing and refocusing delays of 3.75 ms were used. The GARP sequence with a field strength of 3125 Hz was employed for ^{13}C decoupling during ^{1}H acquisition. A total of 256 t_1 values were collected with 592 scans acquired for each t_1 value. The DEPT-HMQC spectrum was acquired on a AMX500 spectrometer with a ^{13}C frequency of 125.76 MHz and the ^{13}C spectral width set to 8804 Hz around the carrier position at 70 ppm relative to internal TSP. For each t_1 value two FIDs with the third ^{1}H pulse alternated between 180° and 0° were recorded (Kessler et al., 1989). To select for CH_2 groups or detect the usual HMQC spectrum, the two FIDs of each t_1 value were added or subtracted, respectively, before Fourier transformation. The GARP sequence with a field strength of 3125 Hz was used for ^{13}C decoupling during ^{1}H acquisition. A total of 219 t_1 values were collected with 256 scans acquired for each t_1 value.

Data were processed either on a Sun Sparc station 2 or on a Silicon Graphics 4D/35 personal Iris computer using Felix software (Hare Research, Inc.). If necessary, low-frequency deconvolution (Marion et al., 1989) was applied to the acquisition dimension to remove the water signal. Typically, the data were zero-filled once in the t_1 dimension and multiplied with a $\pi/3$-, $\pi/4$-, or $\pi/5$-shifted squared sine bell apodization function in both dimensions prior to Fourier transformation. A polynomial base line correction was systematically applied to the rows of the transformed matrices. If necessary, an additional base line correction program was applied to the frequency domain data (Chylla & Markley, 1993). Data were analyzed with the EASY program package (Eccles et al., 1991).

RESULTS

The single *N*-linked glycosylation site in hu-sCD2$_{105}$ at Asn65 is occupied with only high-mannose oligosaccharides when recombinant hu-sCD2$_{182}$ is expressed in CHO cells

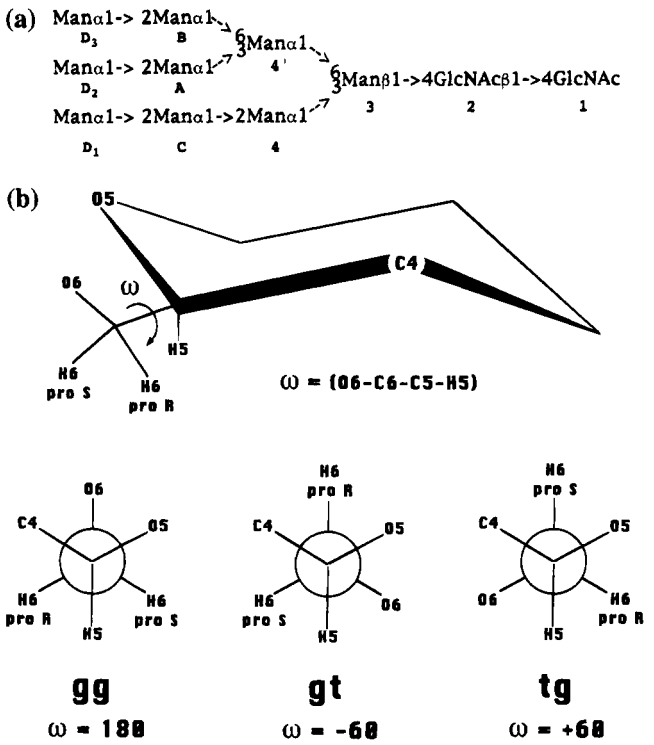

FIGURE 1: (a) Man_9 glycomer from which the glycomers present in our sample originate by trimming at the three branch points. The notation is taken from Vliegenthart et al. (1983). (b) Definition of the dihedral angle ω as used in this work. Values of ω are given in parentheses for the gauche−gauche (gg), gauche−trans (gt), and trans−gauche (tg) rotamers.

(Recny et al., 1992). Although the exact carbohydrate glycotype of CD2 on human T cells is not known, the glycosylation pattern for human CD2 expressed in CHO cells is presumably similar to that found in humans (Withka et al., 1993). The high-mannose glycan in our samples of hu-$sCD2_{105}$ is composed of heterogeneous isomeric structures (glycomers) containing predominantly Man_5 (~20%), Man_6 (~34%), Man_7 (~40%), and Man_8 (~6%) glycoforms as determined by electrospray ionization mass spectrometry (ESI-MS) (Withka et al., 1993). The glycomers present in our sample arise from trimming the Man_9 oligosaccharide (Figure 1) at different branch points.

Although the number of ^1H resonances in oligosaccharides is relatively low compared to proteins or nucleic acids, the assignment of such resonances is complicated by the fact that the vast majority appears in a very small spectral width (~3.5−4.0 ppm) with consequent overlap problems. An additional complication is found in oligomannose-type oligosaccharides since the large degree of symmetry and repeating structure causes severe cross-peaks overlap. Exceptions are the anomeric protons which resonate at lower field (~4.4−5.2 ppm) due to the electron-withdrawing properties of the ring oxygen. As a consequence, the assignment strategy for oligosaccharides is usually based on these resolved anomeric ^1H resonances [for example, Homans (1990)]. However, in glycoproteins these anomeric ^1H resonances are usually overlapped with H^α resonances from the protein, and hence, the anomeric region in 2D $^1H-^1H$ spectra is complicated by the appearance of large numbers of cross-peaks arising from the spin systems of amino acid residues, such as serines, threonines, and glycines. In contrast, the increased spectral width in ^{13}C NMR results in a much improved dispersion of saccharide resonances in ^{13}C NMR spectra. In addition, most of the carbohydrate ^{13}C resonances lie at different frequency positions than those of the protein [compare, for example, Allerhand and Berman (1984a,b) with Howarth and Lilley (1978)], and as a consequence, $^1H-^{13}C$ correlations lie in distinct regions between the aromatic region and the protein $H^\alpha-C^\alpha$ region. In particular, the aglyconic anomeric carbons which are directly bound to two oxygen atoms resonate in a region free of protein resonances (around 100-105 ppm) (see below). Due to these differences in ^1H and ^{13}C chemical shifts, most of the protein and oligosaccharide resonances can easily be distinguished in a $^1H-^{13}C$ HMQC spectrum. Obviously, to achieve NMR assignments for a glycoprotein, it is crucial to differentiate oligosaccharide from protein resonances.

In a first step, carbohydrate spin systems were distinguished from protein spin systems through $^1H-^{13}C$ HMQC spectra at natural abundance and a series of TOCSY spectra with different mixing times. In addition, we assigned H^6 and $H^{6'}$ resonances of the glycan by selecting for CH_2 groups in a DEPT-HMQC spectrum at natural abundance. In a second phase, these spin systems were allocated to specific positions in the heterogeneous high-mannose oligosaccharides by establishing inter-residue through-space (<5 Å) connectivities obtained from NOESY spectra with different mixing times and comparing the resulting carbohydrate ^1H and ^{13}C chemical shifts with data from identical free oligosaccharides. All experiments were largely acquired at two temperatures (25 and 37 °C) to resolve accidental overlap of resonances with the residual water in the D_2O sample. Table 1 summarizes the obtained assignments. Attempts to further verify these assignments by an HMBC experiment at natural abundance, in which we would expect inter-residue cross-peaks between ^1H and ^{13}C resonances by magnetization transfer through the glycosidic bond (Bax & Summers, 1986; Byrd et al., 1987), or an HMQC-TOCSY experiment at natural abundance, in which an additional TOCSY transfer could help to resolve residual ambiguities in ^{13}C assignments from the HMQC spectrum, were unsuccessful due to the low concentration of the hu-$sCD2_{105}$ sample. However, the glycoprotein could not be concentrated further since it aggregates at higher concentrations.

1. Carbohydrate Spin System Identification. Eleven anomeric ^1H resonances were identified through correlations to their directly bound carbons in $^1H-^{13}C$ HMQC spectra at natural abundance (Figure 2a,b). The C^1 carbon of GlcNAc1 is about 20 ppm upfield shifted compared to all other anomeric carbons since it is not bound to a second oxygen atom but to a nitrogen atom instead (Figure 2a). A series of TOCSY spectra with different mixing times (50, 100, 125, 150, 200, and 250 ms) was subsequently employed to correlate each of these anomeric ^1H resonances to other ^1H resonances within a monosaccharide ring (Figure 2c−e). In the TOCSY spectra with mixing times over 125 ms, only few of the protein resonances remained visible (Figure 2e). In contrast, for most of the carbohydrate spin systems it was possible to spin−lock for much longer periods while retaining sufficient sensitivity, indicating that their values of $T_{1\varrho}$ and T_2 are relatively long and, therefore, they are more mobile than most parts of the protein. As an example, the H^α/H^β and $H^\alpha/H^{\beta'}$ cross-peaks of Ser84 which are visible in the TOCSY spectrum with a 50 ms mixing time (Figure 2d) are no longer observed in the 200 ms spectrum where in the same region two H^1/H^5 cross-peaks of ManC and ManD3 have evolved instead (Figure 2e). In the spectrum with a 125 ms mixing time, however, the latter two cross-peaks are

Table 1: Chemical Shifts of the ^1H and ^{13}C NMR Carbohydrate Resonances of hu-sCD2$_{105}$ at 37 °C, pH 4.5[a]

residue	H^1	H^2	H^3	H^4	H^5	H^6, $H^{6'}$
	C^1	C^2	C^3	C^4	C^5	C^6
GlcNAc1	4.95 (5.01)	3.72 (3.82)	3.57 (3.68)	3.46 (3.46)	2.25 (3.59)	*3.69, 3.82*
	79.43 (79.48)	53.86 (54.97)	73.42 (74.18)	80.84 (80.76)	76.96 (77.52)	*60.89* (61.47)
GlcNAc2	4.40 (4.59)	3.62 (3.78)	*3.61* (3.62)	3.62	3.55	*3.69, 3.82*
	103.24 (102.65)	55.46 (56.30)	*73.53* (73.36)	80.41 (80.04)	75.27 (75.82)	*60.89* (61.34)
Man3	4.75 (4.76)	4.20 (4.23)	3.71 (3.73)	3.85	3.59 (3.62)	3.70, 4.00 (3.77, 3.95)
	101.48 (101.58)	71.14 (71.56)	81.84 (82.09)	*66.02* (66.91)	75.34 (75.71)	66.54 (67.31)
Man4	5.33 (5.33)	4.11 (4.10)	3.99 (4.00)	3.67 (3.68)	3.78 (3.80)	*3.74, 3.89*
	101.81 (102.10)	79.35 (79.67)	*71.07* (71.51)	*67.79* (68.50)	*74.43* (74.77)	*62.01* (62.55)
ManC	5.04 (5.05)	4.06 (4.08)	3.84 (3.85)	3.74	3.65	*3.74, 3.88*
	103.26 (103.50)	*71.00* (71.39)	*71.45* (71.81)	*67.71* (68.20)	*73.53* (74.55)	*62.01* (62.45)
Man4′	4.85 (4.85)	4.10 (4.16)	3.86 (3.91)	*3.85* (3.85)	3.81 (3.79)	3.75, 3.97 (3.70, 4.01)
	100.71 (101.24)	70.42 (70.86)	79.48 (80.02)	*66.74* (67.02)	72.23 (72.50)	66.35 (66.91)
ManA(+D2)	5.39 (5.40)	4.08 (4.10)	*3.98* (3.68)	*3.69*	*3.74*	*3.74, 3.88*
	101.61	79.63	*71.02*	*67.97*	*74.24*	*62.01*
ManA(−D2)	5.09 (5.08)	4.05 (4.08)	3.88 (3.88)	3.75	3.66	*3.74, 3.88*
	103.17 (103.56)	*71.00* (71.56)	71.33 (71.85)	*67.71* (68.32)	*73.66* (74.63)	*62.01* (62.55)
ManB(+D3)	5.13 (5.14)	4.00 (4.03)	3.93 (3.93)	3.68 (3.68)	*3.78*	*3.74, 3.88*
	99.07 (99.37)	79.56 (79.87)	71.28 (71.70)	*67.90* (68.37)	*74.36* (74.08)	*62.01* (62.45)
ManB(−D3)	4.90 (4.90)	3.96 (3.98)	3.82 (3.84)	*3.74* (3.75)	3.67	*3.74, 3.88*
	100.26 (100.60)	*70.94* (71.37)	*71.80* (72.05)	*67.71* (68.18)	*73.72* (74.02)	*62.01* (62.43)
ManD3	5.02 (5.04)	4.05 (4.08)	3.83 (3.84)	3.74 (3.74)	3.62	*3.74, 3.88*
	103.22 (103.50)	*71.00* (71.39)	*71.45* (71.81)	*67.71* (68.20)	*73.53* (74.55)	*62.01* (62.45)
residue	H^{N2}	H(Ac)	C(Ac)			
GlcNAc1	7.37 (8.19)	2.03 (1.99)	23.70 (23.48)			
GlcNAc2	8.02 (8.38)	2.01 (2.05)	24.18 (23.62)			

[a] Chemical shifts are in parts per million (ppm) referenced to TSP and are accurate to ±0.01 ppm. Reference values in parentheses are from Wormald et al. (1991), Allerhand and Berman (1984b), and Dijkstra et al. (1983). Chemical shifts that could not be determined accurately due to overlap are shown in *italic*. Many of the 4 and 5 assignments were distinguished on the basis of reference values found in the literature (see text).

overlapped with the H^{α}/H^{β} cross-peak of Ser84 (Figure 2c).

If one of the couplings around the sugar ring is very small, it essentially blocks the Hartmann−Hahn flow of magnetization during the spin−lock in TOCSY experiments. In oligosaccharides $J_{2,3}$ and $J_{1,2}$ were found to be 3.8 and 0.8 Hz for β-mannose residues and 3.8 and 1.6 Hz for α-mannose residues, respectively (Vliegenthart et al., 1983; Brockbank & Vogel, 1990). As a consequence, for the β-mannose Man3 in hu-sCD2$_{105}$, only a weak H^1/H^2 cross-peak arose with mixing times of 125 ms and longer and no further transfer to any of the other resonances within the ring was observed (Figure 2c,e). With a spin−lock time of 50 ms, most α-mannoses showed only H^1/H^2 cross-peaks and additional cross-peaks were absent or only weak (Figure 2d). However, with increasing mixing times, magnetization from their anomeric protons was often transferred all the way to their H^5 protons and, hence, H^1/H^3, H^1/H^4, and H^1/H^5 cross-peaks were observed (Figure 2c,e). Since the mannose residues have large $J_{3,4}$ and $J_{4,5}$ coupling constants the magnetization transfer from the H^3 to the H^5 protons occurs rapidly and the H^1/H^3, H^1/H^4, and H^1/H^5 cross-peaks appeared simultaneously in the TOCSY spectra with longer mixing times. In contrast to mannose residues, GlcNAc residues have large couplings (6−9 Hz) all around the sugar ring (Inagaki et al., 1989), and consequently, for GlcNAc1 in hu-sCD2$_{105}$ very efficient magnetization transfer from H^1 to H^5 was observed even in TOCSY spectra with short spin−lock duration (Figure 2d). The same is probably true for GlcNAc2, but the four cross-peaks are not resolved because the H^2, H^3, H^4, and H^5 resonances exhibit similar chemical shifts for this residue (Figure 2c). The $H^3(F2)/H^1(F1)$ cross-peaks of all mannose residues exhibited a characteristic doublet fine structure along F2 due to their resolved large $J_{3,4}$ and unresolved small $J_{2,3}$ couplings and, therefore, were easily distinguished from the $H^4(F2)/H^1(F1)$ and $H^5(F2)/H^1(F1)$ cross-peaks which showed a triplet and an unresolved fine structure, respectively (data not shown). Because in GlcNAc residues the $J_{1,2}$, $J_{2,3}$, $J_{3,4}$, and $J_{4,5}$ are all about 10 Hz, the $H^2(F2)/H^1(F1)$, $H^3(F2)/H^1(F1)$, and $H^4(F2)/H^1(F1)$ cross-peaks of GlcNAc1 appeared as triplets along F2. For most residues the distinction between H^2, H^3, H^4, and H^5 resonances was confirmed and in some cases extended through the $^1H-^{13}C$ HMQC spectra after their sequential assignment had been established (see below).

Due to their proximity only 1,2-equatorial−axial, 1,3-diaxial, and 1,5-diaxial proton pairs will produce strong intraresidue cross-peaks to well-resolved anomeric protons in pyranosyl rings. As a consequence, the β-mannose Man3 and the two GlcNAc residues in hu-sCD2$_{105}$ showed strong H^1/H^2, H^1/H^3, and H^1/H^5 NOESY cross-peaks, whereas all the α-mannose residues exhibited only strong H^1/H^2 NOEs (Figure 3).

In contrast to the well-resolved anomeric protons, most other carbohydrate ^1H resonances were heavily overlapped in the region between 3.5 and 4.1 ppm. Only H^4 and H^5 of GlcNAc1 and H^2 of Man3 were separated from this bulk of sugar resonances. In particular, the H^5 of GlcNAc1 has a very unusual chemical shift since it is located close to the aromatic ring of Phe63 of the protein (see below). The resolved H^2 resonance of Man3 was fortunate and enabled us to unambiguously assign the H^3, H^4, and H^5 resonances upon the basis of the H^2/H^3, H^2/H^4, and H^2/H^5 cross-peaks in the TOCSY spectra.

Usually the H^6 protons in oligosaccharides relax very quickly (Inagaki et al., 1989), and hence, no H^1/H^6 cross-peaks were observed in any of the TOCSY spectra of hu-sCD2$_{105}$. However, to achieve sequence specific assignments based upon NOESY spectra, it was essential to assign the H^6 and $H^{6'}$ resonances involved in the two α1−6 glycosidic linkages present in the high-mannose oligosaccharides. In oligosaccharides the TQF-COSY experiment has often proved useful for assigning the H^6 and $H^{6'}$ resonances (Homans, 1990). However, this experiment is insensitive due to the filter and the multiplet structure of the

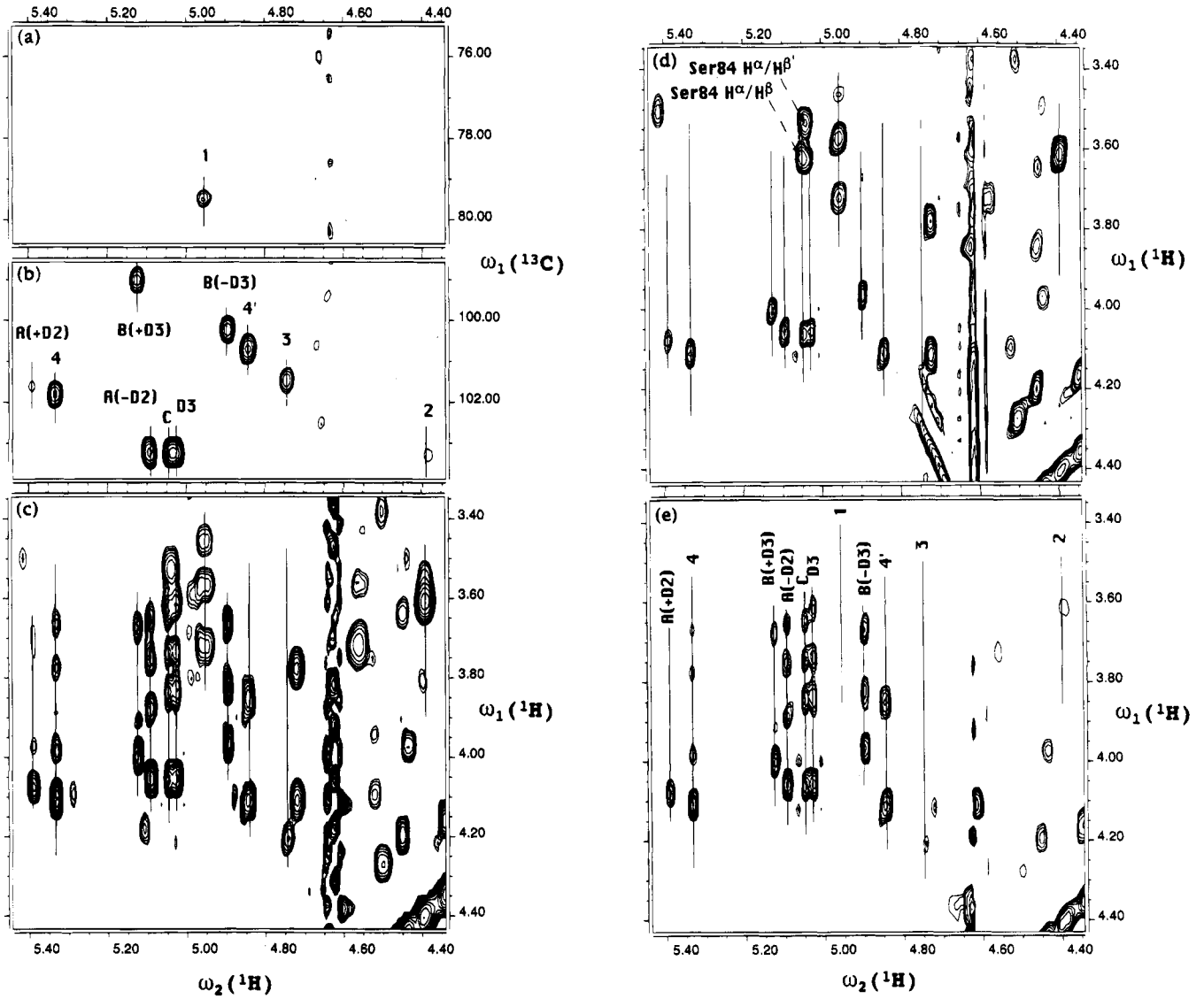

FIGURE 2: (a) Part of a $^1H-^{13}C$ HMQC spectrum of hu-sCD2$_{105}$ at natural abundance recorded in D_2O at 37 °C, pH 4.5, showing the H^1/C^1 correlation of GlcNAc1. (b) Part of the same $^1H-^{13}C$ HMQC spectrum showing the other 10 anomeric proton−carbon correlations which were observed for the high-mannose *N*-glycan of hu-sCD2$_{105}$. (c−e) Part of representative TOCSY spectra of hu-sCD2$_{105}$ acquired under identical conditions to panel a using spin−lock times of 125 ms (c), 50 ms (d), and 200 ms (e) and showing most of the observed H^1/H^2, H^1/H^3, H^1/H^4, and H^1/H^5 cross-peaks (see Table 1 for the chemical shift assignments). (Note that the spectrum in panel c was acquired with 4 times the number of scans per t_1 value than the spectra in panels d and e.) The 11 carbohydrate spin systems detected in the NMR sample of hu-sCD2$_{105}$ are indicated by continuous vertical lines at the chemical shift position of their anomeric H^1 resonances. For the notation of the carbohydrate residues, refer to Figure 1. The H^α/H^β and $H^\alpha/H^{\beta'}$ cross-peaks of Ser84 are indicated in panel d which are no longer visible in the TOCSY spectrum with a 200 ms mixing time (e) where the two H^1/H^5 cross-peaks of ManC and ManD3 are observed instead.

resulting cross-peaks that can pass the triple-quantum filter. This antiphase splitting could lead to cancellation of cross-peaks due to large line widths and severe overlap problems in glycoproteins such as hu-sCD2$_{105}$. As a consequence, we employed a DEPT-HMQC experiment at natural abundance to achieve the assignment of the H^6 and $H^{6'}$ sugar resonances. This experiment is also relatively insensitive, but the selected cross-peaks are in phase and dispersed in the first dimension by their ^{13}C chemical shifts. Due to the electron-withdrawing properties of the oxygen, the C^6 resonances of Man3 and Man4′ which are involved in the two α1−6 glycosidic linkages resonate at lower field (~4.5 ppm) than those of the other mannose residues and the serine C^β resonances (boxes H and I in Figure 4a) and, consequently, their H^6 and $H^{6'}$ resonances were readily distinguished from protein CH_2 groups in the DEPT-HMQC spectrum. The H^6 and $H^{6'}$ resonances of all other mannose residues were overlapped causing two very strong unresolved C^6/H^6 and $C^6/H^{6'}$ cross-peaks. The C^6 resonances of the two GlcNAc residues were further upfield shifted by about 1 ppm with respect to the C^6 resonances of the mannose residues.

The $N^\delta H$ of Asn65 and the NH group of the GlcNAc1 residue were readily assigned in a TOCSY spectrum acquired in H_2O with a 50 ms mixing time in which a strong $N^\delta H/H^1$, a weak $N^\delta H/H^2$, a strong NH/H^2, a weak NH/H^1, and a weak NH/H^3 cross-peak were observed. The NAc group was identified through a strong NAc/NH NOE in a NOESY spectrum acquired in H_2O with a 76 ms mixing time. These assignments were considerably simplified by the fact that the protein resonances had previously been assigned (Wyss et al., 1993). However, in the GlcNAc2 residue these resonances were difficult to detect using the same strategy due to overlap of its NH resonance with many other protein amide resonances.

In summary, using the procedures described above complete spin systems were observed for all but the GlcNAc2

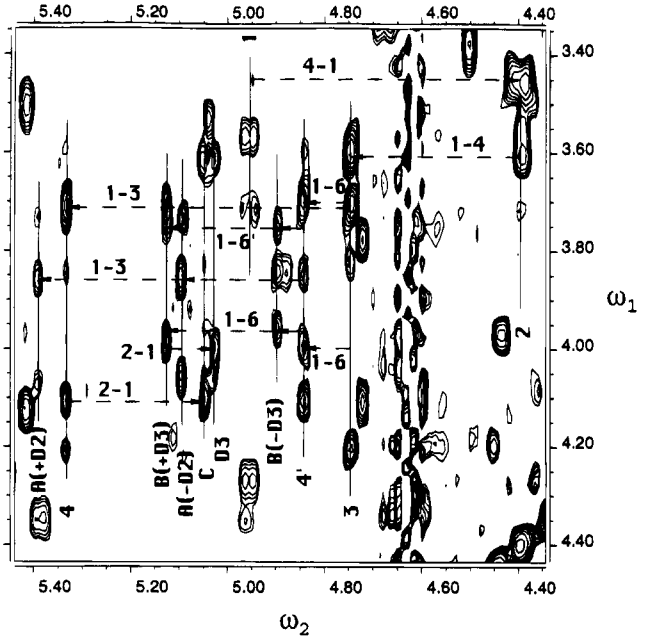

FIGURE 3: Part of a NOESY spectrum of hu-sCD2$_{105}$, recorded in D_2O at 25 °C, pH 4.5, with a mixing time of 100 ms, showing the sequential connectivity pathway for the 11 identified carbohydrate spin systems. For the sake of clarity, only sequential connectivities between the nearest protons across a glycosidic linkage are indicated. Each point of intersection between the end of a horizontal arrow and a vertical line indicates such a sequential connectivity. Due to overlap a few horizontal arrows do not point to centers of gravity of some cross-peaks. However, those sequential NOEs were resolved below the diagonal in NOESY spectra obtained at different conditions and processed with strong resolution enhancement apodization functions along ω_2. The labels should be read in the direction of the arrow, and 2−1, 3−1, 4−1, 6−1, and 6′−1 stand for H^2/H^1, H^3/H^1, H^4/H^1, H^6/H^1, and $H^{6'}/H^1$ cross-peaks, respectively. The residues are labeled as in Figure 2, and the vertical lines are identical to those of Figure 2c−e. Note that Man4′ shows sequential H^3/H^1 connectivities to both ManA(+D2) and ManA(−D2), as well as sequential H^6/H^1 and $H^{6'}/H^1$ connectivities to both ManB(+D3) and ManB(−D3). For the notation of the carbohydrate residues, refer to Figure 1.

and the Man4′(+D3) carbohydrate residues of hu-sCD2$_{105}$ where the H^3 and H^4 resonances could not be distinguished due to overlap. In addition, for many of the sugar residues it was not possible to discriminate between H^4 and H^5 resonances at this point.

2. *Sequential Assignments.* Knowing the composition of the heterogeneous high-mannose *N*-glycan from the ESI-MS measurements and having previously assigned the protein resonances (Wyss et al., 1993) clearly simplified the task of sequentially assigning the carbohydrate resonances. Moreover, most of the carbohydrate resonances are much narrower when compared with resonances of the protein and the rest of the glycan. In accordance, these sharp carbohydrate resonances belong to spin systems which remain visible in TOCSY spectra with prolonged mixing times. This suggests that part of the glycan is mobile and the interaction between the protein and the carbohydrate is limited to a few sugar residues. Hence, we anticipated that the high-mannose *N*-glycan of hu-sCD2$_{105}$ exhibits ^1H and ^{13}C chemical shifts and NOE data very similar to free oligosaccharides with identical composition to the glycomers present in our hu-sCD2$_{105}$ sample. Several NOESY spectra and $^1H-^{13}C$ HMQC spectra at natural abundance of hu-sCD2$_{105}$ were obtained and compared with NOE and ^1H and ^{13}C chemical shift data of free high-mannose oligosaccharides reported in

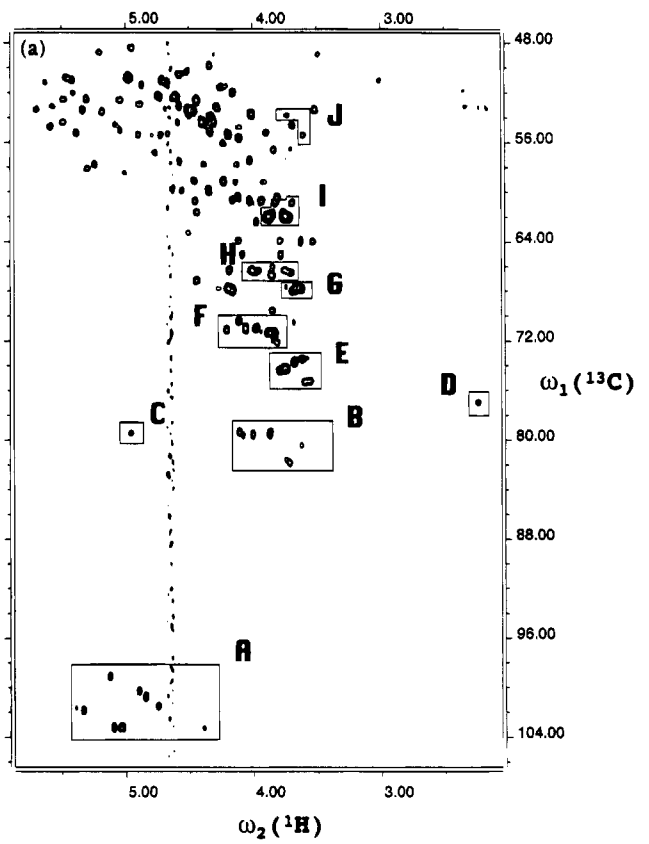

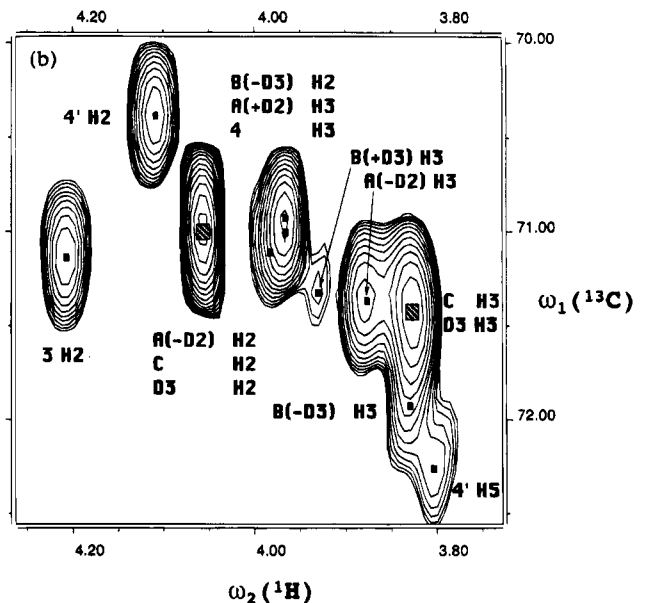

FIGURE 4: (a) Part of the same $^1H-^{13}C$ HMQC spectrum as in Figure 2a,b. All the heteronuclear sugar correlations are highlighted with boxes which include the following correlations: (A) H^1/C^1 of all mannoses and GlcNAc2; (B) H^2/C^2 of Man4, ManA(+D2), and ManB(+D3), H^3/C^3 of Man4′ and Man3, and H^4/C^4 of GlcNAc1 and GlcNAc2; (C) H^1/C^1 of GlcNAc1; (D) H^5/C^5 of GlcNAc1; (E) H^3/C^3 of GlcNAc1 and GlcNAc2 and H^5/C^5 of all residues except GlcNAc1 and Man4′; (F) H^2/C^2 of Man3, Man 4′, ManA(−D2), ManC, ManD3, and ManB(−D3), H^3/C^3 of Man4, ManA(+D2), ManB(+D3), ManA(−D2), ManC, ManD3, and ManB(−D3), and H^5/C^5 of Man4′; (G) H^4/C^4 of ManA(−D2), ManB(−D3), ManC, ManD3, ManB(+D3), and Man4; (H) H^4/C^4, H^6/C^6, and $H^6/C^{6'}$, of Man3 and Man4′; (I) H^6/C^6, and $H^6/C^{6'}$ of GlcNAc1 and GlcNAc2 and all mannoses except Man3 and Man4′; (J) H^2/C^2 of GlcNAc1 and GlcNAc2. All other cross-peaks represent H^α/C^α and H^β/C^β (Ser and Thr) correlations from the protein. (b) Expansion of box F of panel a. For the notation of the carbohydrate residues, refer to Figure 1.

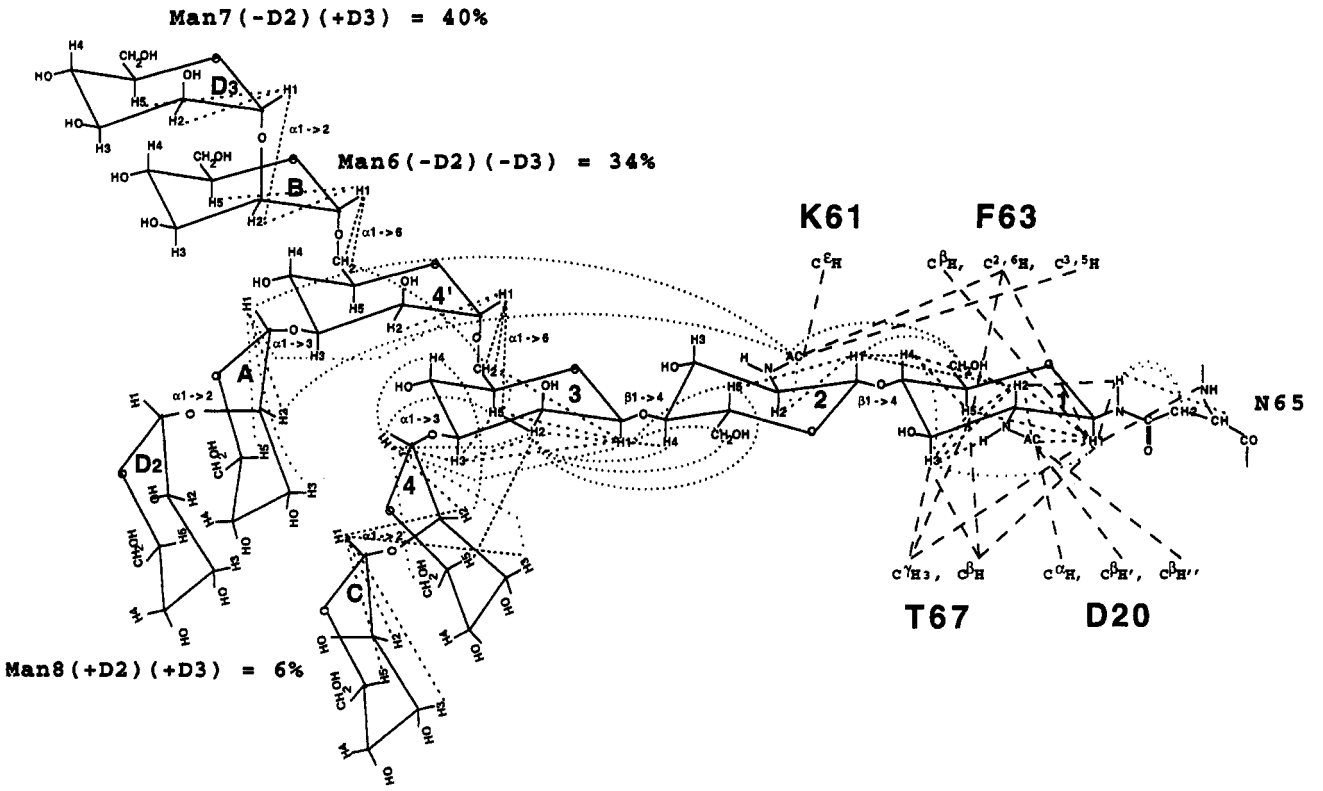

FIGURE 5: Summary of the NOE data obtained for the high-mannose *N*-glycan of hu-sCD2$_{105}$. NOEs are only indicated if they were unambiguously assigned. A lot more NOEs to carbohydrate protons are expected, but they were either not resolved in the NOESY spectra or could not be assigned because many of the H^2, H^3, H^4, H^5, and H^6 sugar resonances exhibit very similar chemical shifts (Table 1). Carbohydrate intraresidue and inter-residue NOEs are shown by dotted lines, and carbohydrate–protein contacts are indicated by dashed lines. Carbohydrate residues are labeled as in Figure 1, and the protein residues are abbreviated by the one-letter codes and residue numbers. The composition and abundance of the glycomers present in our sample as determined by NMR and ESI-MS methods are also contained in the figure. The exact composition of the residual 20% Man$_5$ glycomers was not obtained by either method.

the literature (Wormald et al., 1991; Dijkstra et al., 1983; Allerhand & Berman, 1984b). The 11 observed carbohydrate spin systems of the *N*-glycan in hu-sCD2$_{105}$ were thus readily allocated to their sequence position within the heterogeneous carbohydrate, and the composition of the different glycomers which are present in our hu-sCD2$_{105}$ sample was determined. Figures 3 and 4 show representative NOESY and $^1H-^{13}C$ HMQC spectra of hu-sCD2$_{105}$, respectively, Figure 5 summarizes the NOE data and indicates the determined composition of the different glycomers, and Table 1 compares ^1H and ^{13}C chemical shifts of the heterogeneous high-mannose *N*-linked glycan of hu-sCD2$_{105}$ with literature data of free oligosaccharides.

The carbohydrate spin system containing the NH–CH–CH–NH scalar connectivities is unique and therefore was assigned to the GlcNAc1 residue. Several NOE contacts between GlcNAc1 and Asn65, the site of attachment, confirmed this assignment. Moreover, the H^1/C^1 correlation of GlcNAc1 is diagnostic for this residue (Figure 2a and box C in Figure 4a). In the $^1H-^{13}C$ HMQC spectra all the cross-peaks of this residue were easily identified on the basis of the determined ^1H and expected ^{13}C chemical shifts. As a consequence, the H^3, H^4, and H^5 resonances of this spin system were readily distinguished.

We expected a strong inter-residue NOE between the H^4 of GlcNAc1 (3.46 ppm) and the H^1 of GlcNAc2. Such a cross-peak was observed to the carbohydrate spin system whose anomeric ^1H resonates at 4.40 ppm (Figure 3). Unfortunately, this cross-peak was overlapped with the αH/αH′ NOE of Gly66. However, at 4.40 ppm an additional weak NOE to the H^2 of GlcNAc1 (3.72 ppm) was identified on the basis of its characteristic triplet fine structure along F2. The assignment of this carbohydrate spin system (4.40, 3.62, and 3.55 ppm) to GlcNAc2 was further established through the readily observed C^2/H^2, C^4/H^4, and C^5/H^5 cross-peaks in the $^1H-^{13}C$ HMQC spectra at the expected positions. The acetyl groups for both GlcNAc1 and GlcNAc2 were identified upon the basis of the H^2/CH_3 and N^2H/CH_3 NOEs and the corresponding $^{13}CH_3/CH_3$ cross-peaks in the $^1H-^{13}C$ HMQC spectra.

The β-linked Man3 is uniquely characterized by its H^2 signal at 4.20 ppm (Vliegenthart et al., 1983), and the distinction between the H^3, H^4, and H^5 resonances of this spin system was easily achieved on the basis of the $^1H-^{13}C$ HMQC spectra. Unfortunately, some of the sequential NOEs between resonances of the GlcNAc2 residue and the anomeric H^1 of Man3 were overlapped with the intraresidue H^1/H^5 NOE of Man3, and as a consequence, they could not unambiguously be assigned in the NOESY spectra (Figure 3). However, several other inter-residue NOEs between these two residues, in particular to the H^2 resonance of Man3, were well documented.

The H^1 and H^2 resonances of terminal (1→2)-linked α-mannose residues are typically around 5.05 and 4.07 ppm, respectively (Vliegenthart et al., 1983). However, the H^1 resonance of an α-(1→2)-linked mannose residue in high-mannose type carbohydrates shifts significantly, to about 5.39 ppm, if an α-(1→2)-linked mannose residue is attached. Due the heterogeneity of the high-mannose *N*-glycan, we therefore expected some of the anomeric H^1 resonances of the α-(1→2)-linked mannose residues to show two separate signals and, hence, two spin systems for the two cases in

which an additional α-(1→2)-linked mannose residue is attached or not. The ratio of the two anomeric H^1 signals would then be a measure of what percentage an additional α-(1→2)-linked mannose is attached to the respective residue (Figure 5).

Several sequential NOEs between Man3 and Man4, together with a strong sequential H^1/H^2 NOE between Man4 and ManC (Figure 3), readily enabled the sequential assignment of the spin systems for the latter two residues. The chemical shift of the H^1 and H^2 resonances of ManC at 5.04 and 4.06 ppm, respectively, are typical for a terminal α-(1→2)-linked mannose group (Vliegenthart et al., 1983), and no additional spin system was observed for the anomeric H^1 of ManC, indicating that there is little or no glycomer present in the high-mannose *N*-glycan with an α-(1→2)-linked ManD1 attached to ManC.

The sequential assignment of the Man4′ spin system was well established through two strong sequential H^1(Man4′)/$H^{6'}$(Man3) and H^1(Man4′)/$H^{6''}$(Man3) NOEs (Figure 3). The H^4 and H^5 resonances of Man4′ were only assigned through the $^1H-^{13}C$ HMQC spectra by exclusion, but the resulting chemical shifts agreed well with those in the literature. Interestingly, a weak sequential NOE between one of the H^6 resonances of Man3 and one of the H^6 resonances of Man4′ was also observed.

The H^3 resonance of Man4′ showed NOEs to two different carbohydrate spin systems (Figure 3). One of the two spin systems had chemical shifts which are characteristic of a terminal α-(1→2)-linked mannose group, and therefore, it was assigned to ManA(−D2). The other spin system was only very weak suggesting that it originates from a glycomer which is a minor component of the high-mannose *N*-glycan. Its H^1 signal at 5.39 ppm resonates close to the anomeric H^1 of Man4 which is an α-(1→3)-linked mannose residue with a terminal α-(1→2)-linked mannose group attached, and thus, it was assigned to ManA(+D2). No sequential NOE from its H^2 resonance to an anomeric H^1 was observed suggesting that ManD2 is not present in high enough quantity to be detected in the NMR spectra.

Also the H^6 and $H^{6'}$ resonances of Man4′ showed NOEs to two different carbohydrate spin systems (Figure 3). The H^1 and H^2 chemical shifts of one of the two spin systems at 4.90 and 3.96 ppm, respectively, correspond well with values found in the literature for terminal α-(1→6)-linked mannose residues, and therefore, it was assigned to ManB(−D3). In accordance, this ManB(−D3) residue did not show a sequential NOE from its H^2 resonance. The other spin system, however, showed a strong NOE from its H^2 resonance to the anomeric H^1 of a yet unassigned carbohydrate spin system. Consequently, the former and the latter spin systems were assigned as ManB(+D3) and ManD3, respectively.

The information about the glycomer composition of the high-mannose *N*-glycan obtained by NMR is in full agreement with the ESI-MS measurements (Withka et al., 1993). No evidence for the presence of a terminal α-(1→2)-linked ManD1 residue attached to ManC was found in the NMR spectra. Therefore, the composition of the Man_8 glycoform, which was determined by ESI-MS as being ~6% present in our sample, corresponds to the glycomer shown in Figure 5. The much lower intensity of the signals of ManA(+D2) when compared to those of ManB(+D3) suggests that in our sample the ManD2 residue is less abundant than the ManD3 residue. Consequently, the Man_7 glycoform which is 40% present in our sample is mainly composed of the Man_8 glycomer minus the ManD2 residue, and the Man_6 glycoform which is 34% abundant represents the Man_8 glycomer with the ManD2 and ManD3 residues removed. The exact composition of the residual 20% Man_5 glycomers could not be determined on the basis of our NMR data.

Once the sequential assignment and the composition of the *N*-glycan were established, we further analyzed the $^1H-^{13}C$ HMQC spectra (Figure 4a,b) taking into account the evaluated ^1H chemical shifts of the carbohydrate together with ^{13}C chemical shifts observed for free carbohydrates with similar or identical composition to the glycomers present in our hu-$sCD2_{105}$ sample (Allerhand & Berman, 1984b). The comparison with the literature data clearly confirmed our sequential assignments (Table 1) and allowed us to extend the ^1H resonance assignments for the GlcNAc2 and Man4′ residues. For the terminal ManA(−D2), ManB(−D3), ManC(−D1), and ManD3 residues, the H^4 and H^5 proton resonances were assigned on the basis of the literature values and according to our NMR data; these assignments may possibly be reversed. Such a reversal would result in slightly different ^{13}C chemical shifts for the C^4 and C^5 carbons of these residues but would not have any impact on the conformational evaluation of the glycoprotein. Most important, all the ^1H resonances across the glycosidic linkages which are essential for an accurate determination of the carbohydrate conformation were unambiguously assigned.

Most interestingly, two NOEs between the acetyl group of GlcNAc2 and both the H^1 and H^2 resonances of ManA(−D2) were identified indicating that for a significant time the arm with the Man4′ residue is folded toward the trisaccharide core (Figure 5). Moreover, these NOEs were not observed for the ManA(+D2) residue. By comparing conformations of different high-mannose glycomers, Wooten et al. (1990) found that the dihedral angle ω of the Manα1−6Manβ linkage exhibits low flexibility with a preference for the $\omega = 180°$ (gg) conformation (Figure 1b) when residue D2 is present and high flexibility with similar populations for the $\omega = 180°$ (gg) and $\omega = -60°$ (gt) conformations when residue ManD2 is absent. In contrast to the gg conformation in which the arm with the Man4′ residue is extended away from the core residues, in the gt conformation this arm is folded toward the trisaccharide core making the contacts with the core residues which we observe in our data.

Having such extensive sets of protein and carbohydrate ^1H resonance assignments in hand, we carefully checked all the NOESY spectra for possible protein−carbohydrate interactions. About 20 NOEs between the first two GlcNAc residues and the protein residues Asp20, Lys61, Phe63, Asn65, and Thr67 were unambiguously assigned (Figure 5). Fifteen additional potential protein−carbohydrate contacts including three NOEs between the second ϵ-proton of Lys61 and the two ϵ-protons of Lys69 were also observed. The chemical shift data and the line widths of the carbohydrate resonances confirm the site of interaction of the *N*-glycan with the protein as defined by the NOE data. Whereas the chemical shifts for most of the ^1H resonances of the *N*-glycan are close to those observed in free model carbohydrates of identical or similar composition to the glycomers present in our sample, the ^1H signals which interact with the protein are generally shifted from these literature values (Table 1 and Figure 5). The H_5 resonance of GlcNAc1, in particular, is upfield shifted by 1.34 ppm which can only be explained by its proximity to the aromatic ring of Phe63. Also the

line widths of the core resonances of the carbohydrate, which are comparable to protein resonances within the protein core, are significantly broader than those of the arm residues of the *N*-glycan indicating their restricted mobility.

From our extensive ^1H and ^{13}C assignments we can now define distinct regions in the $^1H-^{13}C$ spectrum in which the carbohydrate $^1H-^{13}C$ correlations fall (Figure 4a). This characteristic separation of the $^1H-^{13}C$ correlations is readily explained by the covalent structure of the *N*-glycan. Especially, the anomeric carbons are shifted downfield significantly due to the electron-withdrawing effect of the two covalently bound oxygen atoms (box A in Figure 4a). The only exception is the anomeric C^1 of GlcNAc1 at the glycan attachment site which is bound to a nitrogen atom instead (box C in Figure 4a). All nonanomeric $^1H-^{13}C$ correlations involved in glycosidic linkages resonate in region B. The H^3/C^3 correlations of the two GlcNAc residues together with all H^5/C^5 correlations except those of GlcNAc1 and Man4′ fall in region E. The H^5/C^5 correlation of Man4′ is slightly shifted downfield into region F which might be due to the folding of the Man4′-ManA arm toward the trisaccharide core. The very unusual H^5 chemical shift of GlcNAc1 is caused by the proximity of this atom to the aromatic ring of Phe63 (region D). Region F contains all the H^2/C^2 and H^3/C^3 correlations of residues whose C^2 and C^3 atoms, respectively, are not involved in a glycosidic linkage. The H^4/C^4 correlations of all mannose residues whose C^3 is not $\alpha1-3$ linked resonate in region G. The H^4/C^4, H^6/C^6, and $H^{6'}/C^6$ correlations of Man3 and Man4′ fall in region H, and all the other H^6/C^6 and $H^{6'}/C^6$ correlations of residues not involved in $\alpha1-6$ linkages resonate in region I. The H^2/C^2 correlations of the two GlcNAc residues are further upfield shifted because their C^2 atom is not bound to a hydroxyl group but to an acetamido group. Whereas in a glycoprotein regions A−F will usually be free of any protein correlations, the same is not true for regions G−J. H^β/C^β correlations of threonines can fall in regions G−H, H^α/C^α correlations of threonines and H^β/C^β correlations of serines may resonate in region I, and H^α/C^α correlations of residual amino acids may lie in region J.

DISCUSSION

We have presented in this paper ^1H and ^{13}C NMR assignments for all the residues of the high-mannose *N*-glycan in the adhesion domain of human CD2 (hu-sCD2$_{105}$) at natural abundance on the intact glycoprotein. We are not aware that this has been achieved on an intact glycoprotein of this size before. The methodology described takes advantage of the following three facts: first, carbohydrate resonances are much more dispersed in the ^{13}C dimension than they are in the ^1H dimension; second, most of the ^{13}C resonances of oligosaccharides lie in different regions than resonances of the protein; third, attached glycans are usually more mobile than most parts of the protein resulting in longer transverse relaxation times. Through minor modifications the presented strategy could easily be adapted to a specific problem such that not only high-mannose but also hybrid and complex type oligosaccharides could be studied by NMR on the intact glycoprotein. Moreover, if the concentration of a glycoprotein can be increased such that additional heteronuclear $^1H-^{13}C$ experiments at natural abundance or 3D homonuclear experiments become possible, the assignment process could further be simplified. However, if more than one glycan is present in the glycoprotein, the size of the attached oligosaccharide is large, or the carbohydrate resonances are significantly shifted by tertiary interactions with the protein, the task of assigning the sugar resonances may become increasingly problematic.

Only few crystal structures and no complete NMR structure of an intact glycoprotein have been solved to date. In X-ray crystallography, protein glycosylation is often a problem for crystallogenesis (McPherson, 1982) whereby heavy glycosylation may obscure the protein surface, microheterogeneity may prevent the formation of reproducible crystal contacts, or the flexibility of the oligosaccharides may limit the order of the crystals (Davis et al., 1993). To make crystallization of glycoproteins easier, several approaches for preventing the addition of oligosaccharides or for facilitating their removal have been developed which are discussed, for example, in Davis et al. (1993). The same features which make glycoproteins difficult to study by crystallography also complicate their structural characterization by NMR, since heavy glycosylation may drastically complicate resonance assignments or even increase the correlation time of the molecule to such an extent that NMR experiments become impossible. Moreover, microheterogeneity and flexibility of oligosaccharides in glycoproteins can severely complicate NMR assignments as well as the interpretation of conformational information which is contained in the NMR spectra. However, hu-sCD2$_{105}$ comprises only a single high-mannose *N*-glycan composed of a limited number of different glycoforms [(Man)$_n$GlcNAc$_2$, $n = 5-8$] (Figures 1 and 5) when a two-domain CD2 segment (hu-sCD2$_{182}$) is expressed in CHO cells, and parts of this *N*-glycan appear to be well restrained due to interactions with the protein. In addition, extensive protein NMR assignments were previously obtained on the intact glycoprotein (Wyss et al., 1993) which facilitated carbohydrate assignments as well as the detection of contacts between the glycan and the protein. Hence, we achieved complete ^1H and ^{13}C NMR assignments of the carbohydrate resonances of hu-sCD2$_{105}$ (Table 1), determined the composition of the different glycomers which are present in our sample (Figure 5), obtained conformational parameters for the high-mannose *N*-glycan (Figure 5), and revealed its orientation with respect to the protein (Figure 6).

It was previously found that the heterogeneous high-mannose *N*-glycan attached to Asn65 in hu-sCD2$_{105}$ is essential for its adhesion functions (Recny et al., 1992). Analysis of deglycosylated soluble recombinant CD2 as well as nonglycosylated mutant transmembrane CD2 molecules containing single Asn65−Gln65 or Thr67−Ala67 mutations demonstrated that neither deglycosylated CD2 nor the mutant CD2 transmembrane receptors bound CD58 or monoclonal antibodies directed at native CD2 adhesion domain epitopes (Recny et al., 1992; Arulanandam et al., 1993). On the basis of our extensive protein and carbohydrate ^1H resonance assignments which are a prerequisite for a detailed structural description of the carbohydrate conformation and its interaction with the protein, we have identified about 20 carbohydrate−protein contacts and a large set of NOEs between ^1H resonances across the glycosidic linkages (Figure 5). Interestingly, we found an extensive network of interactions between the two GlcNAc residues and the amino acid side chains of residues which are solvent exposed on the BED surface of the molecule (Figure 6). However, the CD58 binding site of human CD2 as defined by mutagenesis studies (Arulanandam et al., 1993b; Somoza et al., 1993) involves residues in the β-strands C, C′, F, and G and in the

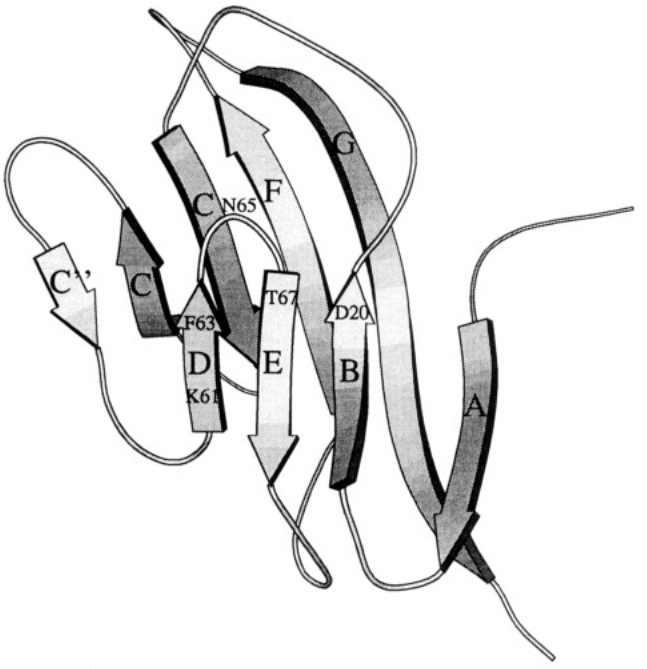

FIGURE 6: Ribbon diagram illustrating the overall fold of hu-sCD2$_{105}$. The recently refined average structure of hu-sCD2$_{105}$ (D. Wyss, J. Choi, M. Knoppers, M. Recny, and G. Wagner, unpublished results) is shown with the β-sheet implicated in CD58 binding (G, F, C, C′, and C″) in the background and the β-sheet with the sugar contact residues (D, E, and B) in the foreground. The high-mannose *N*-glycan is attached to the protein at Asn65 at the top of the DE loop and is oriented toward the β-sheet (DEB) making contact with a number of solvent-exposed side chains of residues within the DEB sheet that are indicated with one-letter codes and residue numbers. [Figure prepared using the MOLSCRIPT program (Kraulis, 1991)].

surrounding loops CC′, C′C″, and FG. This GFCC′C″ face of the glycoprotein is located on the β-sheet opposite to the *N*-glycan, and therefore, it is unlikely that the carbohydrate is directly involved in the contact with CD58 (Figure 6). Moreover, a previous model suggesting the carbohydrate to fill a cavity between the BC, C′C″, and FG loops on the top of the Ig-like β-barrel (Withka et al., 1993) has not been confirmed by our new data. We did not observe any interactions of carbohydrate residues from the branches with the protein, and in addition, branch residues exhibited narrower line widths than the trisaccharide core (GlcNAc1-GlcNAc2-Man3) or most of the protein implying their higher mobility. These findings together with the recent crystal structure of two-domain human CD2 (Bodian et al., 1994) suggest that the first GlcNAc residue is sufficient for stability and *in vitro* adhesion function of the protein. The latter protein was expressed in CHO cells in the presence of a glucosidase I inhibitor which produced truncated *N*-linked oligosaccharides that were trimmed by endoglycosidase H resulting in human CD2 with single GlcNAc residues at each glycosylation site. Therefore, it seems possible that the carbohydrate is just needed to ensure the correct folding of the polypeptide and can be removed subsequently without affecting the stability or the adhesion function of the protein. On the other hand, the carbohydrates could be important *in vivo*, for instance, during conjugate formation when CD2 molecules are reorganized into the cell−cell interaction site (Koyasu et al., 1990). The oligosaccharides in human CD2 may also be involved in molecular recognition events, signal transduction after receptor binding, or modifying the local structure and overall dynamics of the glycoprotein.

Most interestingly, two medium-range NOEs were identified between both the H^1 and H^2 resonances of ManA-(−D2) (Figure 5) and the acetyl protons of GlcNAc2 indicating that a conformation in hu-sCD2$_{105}$ is significantly populated where one arm of the high-mannose *N*-glycan is folded toward the trisaccharide core. To our knowledge this is the first time that direct experimental evidence has been observed which suggests this folding of the Man4′-ManA-(−D2) arm. However, upon the basis of a detailed comparison of spin−spin coupling and chemical shift data for a series of high-mannose oligosaccharides, Wooten et al. (1990) determined the rotamer distributions about the dihedral angle ω for the Man4′(α1→6)Man3 and ManB-(α1→6)Man4′ linkages for each member of the series. They concluded from these studies that the dihedral angle ω of the Man4′(α1→6)Man3 linkage exhibits low flexibility with a preference for the $\omega = 180°$ conformation ($P_{-60}/P_{180} \approx 20/80$) when residue D2 is present and high flexibility ($P_{-60}/P_{180} \approx 40/60$) when this residue is absent. They also found that the flexibility of ω for the ManB(α1→6)Man4′ linkage is intermediate between the two Man4′(α1→6)Man3 extremes with a preference for the $\omega = 180°$ conformation ($P_{-60}/P_{180} \approx 30/70$) and is largely independent of primary sequence. Due to an unfavorable synperiplanar repulsion between O4 and O6 (Hassel−Ottar effect), the $\omega = 60°$ conformer is destabilized and, consequently, is not significantly populated in high-mannose glycans. On the basis of molecular modeling together with chemical and enzymatic modification studies, they rationalized that these differences in rotamer populations arise from steric factors. They observed that when $Man_9GlcNAc_2$ is in the ω(Man4′(α1→6)-Man3),(ManB(α1→6)Man4′) (180°,180°) conformation, the arms and core are spread apart and do not interact significantly with each other. However, in the −60°,180° conformation, ManD2 makes unfavorable contacts with GlcNAc1 and to a lesser extent with GlcNAc2, and hence, the $\omega = -60°$ conformation is less stable when ManD2 is present. Here, we observe NOEs between the ManA(−D2) residue and the GlcNAc2 residue, but we do not detect these NOEs when ManD2 is present. However, having only about 6% Man_8 glycomer with ManD2 in our sample may prevent the detection of possible existing contacts to the core residues. We clearly do not observe any interaction between the outer arm residue ManB and the core residue GlcNAc2 as proposed by molecular dynamics (MD) simulations for a model of Man_5 with the inner 1→6 linkage in the gt conformation (Woods et al., 1994).

It was previously postulated that recognition of individual oligomannose conformations may play a role in the control of *N*-linked oligosaccharide biosynthesis (Wooten et al., 1990). Moreover, oligosaccharides in secreted and cell surface glycoproteins and cell surface glycolipids are known to change during developmental and transformational events. In this regard, glycosidases and glycosyltransferases may only process certain carbohydrate structures if they recognize specific conformations of the oligosaccharides which might be important for the transport of glycoproteins (van den Eijnden et al., 1985; Lubas & Spiro, 1988). The folding of the Man4′-ManA(−D2) arm toward the trisaccharide core (GlcNAc1-GlcNAc2-Man3) might be one of the reasons for the observed branch specificity of certain enzymes.

Several detailed studies have been undertaken on the characterization of the extent of internal motions in free oligosaccharides [for example, Cumming et al. (1987),

Cumming and Carver (1987), Breg et al. (1988), Edge et al. (1990), Rutherford et al. (1993), Pérez (1993), Woods et al. (1994)]. However, there is currently much debate regarding the extent and nature of internal motions in oligosaccharides although the conformational flexibility of oligosaccharides in general is becoming more widely acknowledged. In fact, while the qualitative picture can reliably be derived from NMR, the detailed picture must necessarily depend for the most part on theoretical energy calculations and molecular dynamics simulations including solvent. Reliable calculations are only now becoming available on free model compounds (Edge et al., 1990; Rutherford et al., 1993; Woods et al., 1994).

Efforts are currently under way to determine the 3D structure of the complete glycoprotein. These calculations may reveal the details of the intramolecular interaction between the high-mannose *N*-glycan and the polypeptide and may give some insight into the function of the attached oligosaccharide. It can be anticipated from this study that also other NMR structures of glycoproteins may become available in the future which might help in understanding the essence of oligosaccharides for the function of glycoproteins. However, a prerequisite for a detailed structural characterization of glycoproteins by NMR is extensive NMR assignments which should become less difficult to achieve as the NMR techniques for the study of biomacromolecules progress.

ACKNOWLEDGMENT

The authors would like to thank M. Knoppers and Dr. M. Recny for providing a highly purified hu-sCD2$_{105}$ sample in D_2O which enabled the NMR studies at natural abundance. We would also like to acknowledge Dr. K. Chandrasekhar for advice on NMR spectroscopy and Dr. A. Krezel for his support regarding computational matters.

REFERENCES

Allerhand, A., & Berman, E. (1984a) *J. Am. Chem. Soc. 106*, 2400−2412.

Allerhand, A., & Berman, E. (1984b) *J. Am. Chem. Soc. 106*, 2412−2420.

Anil-Kumar, Ernst, R. R., & Wüthrich, K. (1980) *Biochem. Biophys. Res. Commun. 95*, 1−6.

Arulanandam, A. R. N., Moingeon, P., Concino, M. F., Recny, M. A., Kato, K., Yagita, H., Koyasu, S., & Reinherz, E. L. (1993a) *J. Exp. Med. 177*, 1439−1450.

Arulanandam, A. R. N., Withka, J. M., Wyss, D. F., Wagner, G., Kister, A., Pallai, P., Recny, M. A., & Reinherz, E. L. (1993b) *Proc. Natl. Acad. Sci. U.S.A. 90*, 11613−11617.

Arulanandam, A. R. N., Kister, A., McGregor, M. J., Wyss, D. F., Wagner, G., & Reinherz, E. L. (1994) *J. Exp. Med. 180*, 1861−1871.

Barclay, A. N., Birkeland, M. L., Brown, M. H., Beyers, A. D., Davis, S. J., Somoza, C., & Williams, A. F. (1993) *The Leucocyte Antigen Facts Book*, Academic Press, London.

Bax, A., & Summers, M. F. (1986) *J. Am. Chem. Soc. 108*, 2093−2094.

Bierer, B. E., Peterson, A., Barbosa, J., Seed, B., & Burakoff, S. J. (1988) *Proc. Natl. Acad. Sci. U.S.A. 85*, 1194−1198.

Bierer, B. E., Sleckman, B. P., Ratnofsky, S. E., & Burakoff, S. J. (1989) *Annu. Rev. Immunol. 7*, 579−599.

Bodian, D. L., Jones, E. Y., Harlos, K., Stuart, D. I., & Davis, S. J. (1994) *Structure 2*, 755−766.

Braunschweiler, L., & Ernst, R. R. (1983) *J. Magn. Reson. 53*, 521−528.

Breg, J., Kroon-Batenburg, L. M. J., Strecker, G., Montreuil, J., & Vliegenthart, J. F. G. (1988) *Eur. J. Biochem. 178*, 727−739.

Brockbank, R. L., & Vogel, H. J. (1990) *Biochemistry 29*, 5574−5583.

Bromberg, J. S. (1993) *J. Surg. Res. 54*, 258−267.

Brown, S. C., Weber, P. L., & Mueller, L. (1988) *J. Magn. Reson. 77*, 166−169.

Byrd, R. A., Egan, W., Summers, M. F., & Bax, A. (1987) *Carbohydr. Res. 166*, 47−58.

Cavanagh, J., & Rance, M. (1992) *J. Magn. Reson. 96*, 670−678.

Chang, H.-C., Moingeon, P., Lopez, P., Krasnow, H., Stebbins, C., & Reinherz, E. L. (1989) *J. Exp. Med. 169*, 2073−2083.

Chavin, K. D., Qin, L., Lin, J., Yagita, H., & Bromberg, J. S. (1993) *J. Immunol. 151*, 7249−7259.

Chothia, C., Novotny, J., Bruccoleri, R., & Karplus, M. (1985) *J. Mol. Biol. 186*, 651−663.

Chylla, R. A., & Markley, J. M. (1993) *J. Magn. Reson. B 102*, 148−154.

Clayton, L. K., Sayre, P. H., Novotny, J., & Reinherz, E. L. (1987) *Eur. J. Immunol. 17*, 1367−1370.

Cumming, D. A., & Carver, J. P. (1987) *Biochemistry 26*, 6664−6676.

Cumming, D. A., Shah, R. N., Krepinsky, J. J., Grey, A. A., & Carver, J. P. (1987) *Biochemistry 26*, 6655−6663.

Davis, S. J., Puklavec, M. J., Ashford, D. A., Harlos, K., Jones, E. Y., Stuart, D. I., & Williams, A. F. (1993) *Protein Eng. 6*, 229−232.

Deckert, M., Kubar, J., Zoccola, D., Bernard-Pomier, G., Angelisova, P., Horejsi, V., & Bernard, A. (1992) *Eur. J. Immunol. 22*, 2943−2947.

Dijkstra, B. W., Vliegenthart, J. F. G., Strecker, G., & Montreuil, J. (1983) *Eur. J. Biochem. 130*, 111−115.

Driscoll, P. C., Cyster, J. G., Campbell, I. D., & Williams, A. F. (1991) *Nature 353*, 762−765.

Dustin, M. L., & Springer, T. A. (1991) *Annu. Rev. Immunol. 9*, 27−66.

Eccles, C., Güntert, P., Billeter, M., & Wüthrich, K. (1991) *J. Biomol. NMR 1*, 111−130.

Edge, C. J., Singh, U. C., Bazzo, R., Taylor, G. L., Dwek, R. A., & Rademacher, T. W. (1990) *Biochemistry 29*, 1971−1974.

Fletcher, C. M., Harrison, R. A., Lachmann, P. J., & Neuhaus, D. *Structure 2*, 185−199.

Hahn, W. C., Menu, E., Bothwell, A. L. M., Sims, P. J., & Bierer, B. E. (1992) *Science 256*, 1805−1807.

Hahn, W. C., Menu, E., & Bierer, B. E. (1993) in *Lymphocyte Adhesion Molecules* (Shimizu, Y., Ed.) pp 105−134, R. G. Landes Co., Austin, TX.

He, Q., Beyers, A. D., Barclay, A. N., & Williams, A. F. (1988) *Cell 54*, 979−984.

Homans, S. W. (1990) *Prog. Nucl. Magn. Reson. Spectrosc. 22*, 55−81.

Howarth, O. W., & Lilley, D. M. J. (1978) *Prog. Nucl. Magn. Reson. Spectrosc. 12*, 1−40.

Hünig, T., Tiefenthaler, G., Meyer zum Büschenfelde, K.-H., & Meuer, S. C. (1987) *Nature 326*, 298−301.

Inagaki, F., Shimada, I., Kohda, D., Suzuki, A., & Bax, A. (1989) *J. Magn. Reson. 81*, 186−190.

Jeener, J., Meier, B. H., Bachmann, P., & Ernst, R. R. (1979) *J. Chem. Phys. 71*, 4546−4553.

Jones, E. Y., Davis, S. J., Williams, A. F., Harlos, K., & Stuart, D. I. (1992) *Nature 360*, 232−239.

Kato, K., Koyanagi, M., Okada, H., Takanashi, T., Wong, Y. W., Williams, A. F., Okumura, K., & Yagita, H. (1992) *J. Exp. Med. 176*, 1241−1249.

Kessler, H., Schmieder, P., & Kurz, M. (1989) *J. Magn. Reson. 85*, 400−405.

Kieffer, B., Driscoll, P. C., Campbell, I. D., Willis, A. C., van der Merwe, P. A., & Davis, S. J. (1994) *Biochemistry 33*, 4471−4482.

Koyasu, S., Lawton, T., Novick, D., Recny, M. A., Siliciano, R. F., Wallner, B. P., & Reinherz, E. L. (1990) *Proc. Natl. Acad. Sci. U.S.A. 87*, 2603−2607.

Kraulis, P. J. (1991) *J. Appl. Crystallogr. 24*, 946−950.

Leahy, D. J., Axel, R., & Hendrickson, W. A. (1987) *Nature 329*, 506−512.

Lubas, W. A., & Spiro, R. G. (1988) *J. Biol. Chem. 263*, 3990−3998.

Marion, D., & Wüthrich, K. (1983) *Biochem. Biophys. Res. Commun. 113*, 967−974.

Marion, D., Ikura, M., & Bax, A. (1989) *J. Magn. Reson. 84*, 425−428.
McPherson, A. (1982) *Preparations and Analysis of Protein Crystals*, John Wiley & Sons, New York.
Meuer, S. C., Hussey, R. E., Fabbi, M., Fox, D., Acuto, O., Fitzgerald, K. A., Hodgdon, J. C., Protentis, J. P., Schlossman, S. F., & Reinherz, E. L. (1984) *Cell 36*, 897−906.
Miller, G. T., Hochman, P. S., Meier, W., Tizard, R., Bixler, S. A., Rosa, M. D., Wallner, B. P. (1993) *J. Exp. Med. 178*, 211−222.
Moingeon, P., Chang, H.-C., Wallner, B. P., Stebbins, C., Frey, A. Z., & Reinherz, E. L. (1989a) *Nature 339*, 312−314.
Moingeon, P., Chang, H.-C., Sayre, P. H., Clayton, L. K., Alcover, A., Gardner, P., & Reinherz, E. L. (1989b) *Immunol. Rev. 111*, 111−144.
Moingeon, P. E., Lucich, J. L., Stebbins, C. C., Recny, M. A., Wallner, B. P., Koyasu, S., & Reinherz, E. L. (1991) *Eur. J. Immunol. 21*, 605−610.
Mueller, L. (1979) *J. Am. Chem. Soc. 101*, 4481−4484.
Pérez, S. (1993) *Curr. Opin. Struct. Biol. 3*, 675−680.
Pigott, R., & Power, C. (1993) *The Adhesion Molecule Facts Book*, Academic Press, London.
Qin, L., Chavin, K. D., Lin, J., Yagita, H., & Bromberg, J. S. (1994) *J. Exp. Med. 179*, 341−346.
Rabin, E. R., Gordon, K., Knoppers, M. H., Luther, M. A., Neidhardt, E. A., Flynn, J. F., Sardonini, C. A., Sampo, T. M., Concino, M. F., Recny, M. A., Reinherz, E. L., & Dwyer, D. S. (1993) *Cell. Immunol. 149*, 24−38.
Recny, M. A., Neidhardt, E. A., Sayre, P. H., Ciardelli, T. L., & Reinherz, E. L. (1990) *J. Biol. Chem. 265*, 8542−8549.
Recny, M. A., Luther, M. A., Knoppers, M. H., Neidhardt, E. A., Khandekar, S. S., Concino, M. F., Schimke, P. A., Francis, M. A., Moebius, U., Reinhold, B. B., Reinhold, V. N., & Reinherz, E. L. (1992) *J. Biol. Chem. 267*, 22428−22434.
Rutherford, T. J., Partridge, J., Weller, C. T., & Homans, S. W. (1993) *Biochemistry 32*, 12715−12724.
Sayre, P. H., Chang, H.-C., Hussey, R. E., Brown, N. R., Richardson, N. E., Spagnoli, G., Clayton, L. K., & Reinherz, E. L. (1987) *Proc. Natl. Acad. Sci. U.S.A. 84*, 2941−2945.
Sayre, P. H., Hussey, R. E., Chang, H.-C., Ciardelli, T. L., & Reinherz, E. L. (1989) *J. Exp. Med. 169*, 995−1009.
Selvaraj, P., Plunkett, M. L., Dustin, M., Sanders, M. E., Shaw, S., & Springer, T. A. (1987) *Nature 326*, 400−403.
Sewell, W. A., Brown, M. H., Dunne, J., Owen, M. J., & Crumpton, M. J. (1986) *Proc. Natl. Acad. Sci. U.S.A. 83*, 8718−8722.
Shaka, A. J., Lee, C. J., & Pines, A. (1988) *J. Magn. Reson. 77*, 274−293.
Shaw, S., Ginther Luce, G. E., Quinones, R., Gress, R. E., Springer, T. A., & Sanders, M. E. (1986) *Nature 323*, 262−264.
Siliciano, R. F., Pratt, J. C., Schmidt, R. E., Ritz, J., & Reinherz, E. L. (1985) *Nature 317*, 428−430.
Somoza, C., Driscoll, P. C., Cyster, J. G., & Williams, A. F. (1993) *J. Exp. Med. 178*, 549−558.
van den Eijnden, D. H., Blanken, W. M., & van Vliet, Anja (1986) *Carbohydr. Res. 151*, 329−335.
van der Merwe, P. A., McPherson, D. C., Brown, M. H., Barclay, A. N., Cyster, J. G., Williams, A. F., & Davis, S. J. (1993a) *Eur. J. Immunol. 23*, 1373−1377.
van der Merwe, P. A., Brown, M. H., Davis, S. J., & Barclay, A. N. (1993b) *EMBO J. 12*, 4945−4954.
van der Merwe, P. A., Barclay, A. N., Mason, D. W., Davies, E. A., Morgan, B. P., Tone, M., Krishnam, A. K. C., Ianelli, C., & Davis, S. J. (1994) *Biochemistry 33*, 10149−10160.
Veitch, N. C., Williams, R. J. P., Bray, R. C., Burke, J. F., Sanders, S. A., Thorneley, R. N. F., & Smith, A. T. (1992) *Eur. J. Biochem. 207*, 521−531.
Vliegenthart, J. F. G., Dorland, L., & van Halbeek, H. (1983) *Adv. Carbohydr. Chem. Biochem. 41*, 209−374.
Wagner, G., & Wyss, D. F. (1994) *Curr. Opin. Struct. Biol. 4* (in press).
Williams, A. F., & Barclay, A. N. (1988) *Annu. Rev. Immunol. 6*, 381−406.
Williams, A. F., Davis, S. J., He, Q., & Barclay, A. N. (1989) *Cold Spring Harbor Symp. Quant. Biol. 54(2)*, 637−647.
Withka, J. M., Wyss, D. F., Wagner, G., Arulanandam, A. R. N., Reinherz, E. L., & Recny, M. A. (1993) *Structure 1*, 69−81.
Woods, R. J., Edge, C. J., & Dwek, R. A. (1994) *Nature Struct. Biol. 1*, 499−501.
Wooten, E. W., Bazzo, R., Edge, C. J., Zamze, S., Dwek, R. A., & Rademacher, T. W. (1990) *Eur. Biophys. J. 18*, 139−148.
Wormald, M. R., Wooten, E. W., Bazzo, R., Edge, C. J., Feinstein, A., Rademacher, T. W., & Dwek, R. A. (1991) *Eur. J. Biochem. 198*, 131−139.
Wyss, D. F., Withka, J. M., Knoppers, M. H., Sterne, K. A., Recny, M. A., & Wagner, G. (1993) *Biochemistry 32*, 10995−11006.
Yang, S. Y., Chouaib, S., & Dupont, B. (1986) *J. Immunol. 137*, 1097−1100.

BI942428E